Threading Dynamics of Ring Polymers in a Gel

Davide Michieletto,[†] Davide Marenduzzo,[‡] Enzo Orlandini,[§] Gareth P. Alexander,[†] and Matthew S. Turner*,[†]

[†]Department of Physics and Complexity Centre, University of Warwick, Coventry CV4 7AL, United Kingdom
[‡]School of Physics and Astronomy, University of Edinburgh, Mayfield Road, Edinburgh EH9 3JZ, Scotland, United Kingdom
[§]Dipartimento di Fisica e Astronomia and Sezione INFN, Università di Padova, Via Marzolo 8, 35131 Padova, Italy

S *Supporting Information*

ABSTRACT: We perform large scale three-dimensional molecular dynamics simulations of unlinked and unknotted ring polymers diffusing through a background gel, here a three-dimensional cubic lattice. Taking advantage of this architecture, we propose a new method to unambiguously identify and quantify inter-ring threadings (penetrations) and to relate these to the dynamics of the ring polymers. We find that both the number and the persistence time of the threadings increase with the length of the chains, ultimately leading to a percolating network of inter-ring penetrations. We discuss the implications of these findings for the possible emergence of a topological jammed state of very long rings.
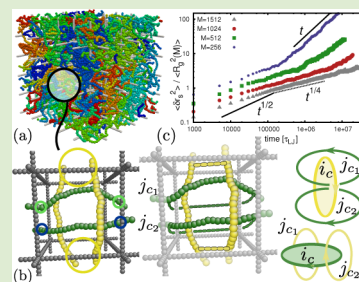
nderstanding the dynamical and rheological properties of solutions of long polymers is of primary importance in several areas of soft matter, material science, and biophysics.[1] The dynamics of linear polymers in the melt is now understood using the tube and reptation models.[2,3] These models take advantage of the topological constraint represented by the noncrossability of the chains to describe the diffusion of the polymers along their own primitive path, by relaxing the free ends. By contrast, the dynamics of ring polymers, which have no free ends, can differ markedly from those of their linear or branched cousins in the melt,[4−14] involving fundamentally different modes of stress relaxation,[9] significantly different diffusion constants,[13,14] and a crossover to free diffusion that occurs only once they traveled many times their own size $\langle R_g^2 \rangle^{1/2}$.[15] Inter-ring penetrations, or "threadings", have previously been speculated to play some role in ring dynamics,[9,11,15−19] although no methodology to define or identify them yet exists. The goal of this work is to study a system in which we can quantify these threadings and their effect on the long-time dynamics of a concentrated solution of ring polymers. At present its not possible to identify such threadings in the melt. Here we focus our attention on a system that is rather different from a melt of rings: We study a concentrated solution of ring polymers embedded in a physical gel which, for simplicity, we model as a rigid cubic lattice, see Figure 1a. As we show below, this system is well suited to the study of inter-ring penetrations (threadings). It is also highly accessible from an experimental point of view, as it resembles the classical setup used for gel electrophoresis[20,21] of plasmid DNA rings, except that the polymer concentration is taken above overlap and the gel is prepared in order to have a pore size comparable to the polymers' Kuhn length. In this Letter we introduce for the first time a quantitative measure of inter-ring threadings for polymers diffusing in a background gel by using a

novel algorithm that employs the background gel as a reference frame. We can then study the consequences of this on their dynamics. We show that the number of threadings grows linearly with the degree of polymerization M of the chain and that this leads to the emergence of an extended directed network of threadings that includes of order all rings. This network of threadings is associated with the onset of very slow dynamics and we show that the unthreading process drives the emergence of a significant slowing down of the longest rings we are able to study. Finally, we speculate that such a threading-rich state may be a precursor of a topological jammed state for even longer chains, as these threadings provide long-lived "pinning" sites that represent severe topological constraints in the polymers' diffusion.

We study unlinked and unknotted ring polymers diffusing through a background gel (see Figure 1a,b), formed by a perfect cubic lattice, that is, without dangling ends. The novel aspect of this work is in how we are able to identify the role of inter-ring threadings. By neglecting fluctuations of the gel we can direct computational resources most effectively toward simulating the dynamics of the rings themselves. We use a molecular dynamics engine (LAMMPS) to model the Langevin dynamics at fixed volume and constant temperature of N polymer rings with length M moving inside a three-dimensional cubic lattice of total linear size L and lattice spacing l. The ring monomer density is kept constant for all the systems at $\rho = NM/L^3 = 0.1\ \sigma^{-3}$ (on top of this, the density of the gel is 0.06 σ^{-3}). The well-established Kremer-Grest model[22] is used to simulate worm-like chains with noncrossability constraint and excluded volume interaction (see SI for simulation details).
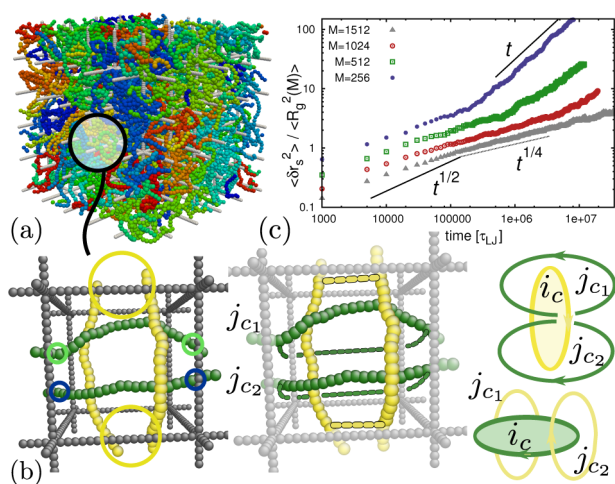
Figure 1. (a) Snapshot of a system with $N = 50$ chains of length $M = 256$. The gel lattice (gray) can be seen to be interpenetrated by ring polymers (various colors). We use periodic boundary conditions so there are no real ends to either the gel or the polymers. (b) Sketch showing our procedure for identifying rings that thread in a given unit cell c of the gel lattice. Here the green strands of chain j passing through a face of the cell (circled) are separately closed to form two loops j_{c_1} and j_{c_2}. Each are topologically linked with the yellow contour i_c, a unique contraction of chain i formed by connecting the points that pass through the faces of the unit cell (circled). In contrast, the green ring is not threaded by the yellow. See text for details. (c) Segmental mean squared displacement of the rings $\langle \delta r_s^2 \rangle = \langle [r_i(t) - r_i(0)]^2 \rangle$ scaled by $\langle R_g^2(M) \rangle$ and plotted against time in units of the Lennard-Jones time $\tau_{LJ} = \sigma (m/\varepsilon)^{1/2}$, where m is the mass of the beads and the target temperature is $T = \varepsilon/k_B$. The gel structure is here thinned for clarity.

The Kuhn length provides a natural choice for the lattice spacing of the gel, $l = l_K = 10\,\sigma$, where σ is the nominal size of a bead composing the polymers. By making this choice, we assume that the mesh size of our idealized gel corresponds to that of a moderately concentrated agarose gel[23] or appropriate DNA hydrogel architecture.[24−26] From a physical perspective, lattice spacings much greater than the Kuhn length can produce a gel so sparse that the rings rarely encounter it. This maps the problem back onto the melt, a different system from the one we study here, and one that is less well suited to the study of inter-ring penetrations. Alternatively, for lattice spacings much shorter than the Kuhn length threadings will ultimately be suppressed by steric effects. Also, the simulation will include an increasingly large fraction of passive gel monomers, which tend to increase the volume fraction of the system and hence limit the concentration of rings that can be studied efficiently using LAMMPS. The choice of $l = l_K = 10\,\sigma$ is a natural compromise and corresponds to systems that can have numerous threadings, as we show below. This is due, at least in part, to the fact that the polymers are forced to spread across many unit cells, and within each cell the polymers are stiff.

We study threadings as local properties of the conformation of rings; the global topology of the rings remains unlinked from both other rings and the gel. Here the gel architecture provides a natural local volume, a single unit cell, within which threading of one ring by another can be identified; no corresponding method exists for the melt. Each polymer enters and exits a given cell through its faces. The unique topological characteristic of ring polymers, unlinked from the cubic lattice, is that each time the contour passes out through a face of any given

unit cell, labeled c, this must be accompanied by a returning passage back through the same cell face. The threading of polymer i by polymer j within cell c can then be defined as follows: First a contraction of ring i is formed by sequentially connecting the points where it passes through any face of cell c by straight lines, as illustrated by the dashed (yellow) lines in Figure 1b. This creates a closed loop (or link) i_c contained entirely within cell c and its bounding faces. In this way we use the gel to identify threadings as local configurations in which the conformation of the ring outside of the chosen cell is unimportant. Next we consider each of the strands, labeled by j_c, of a different polymer j in the same cell c. These strands connect a single entry and exit point through the faces of c. We now close the ends of each strand outside the cell to form a closed loop. We then compute the linking number of the loop thereby created from each j_c with i_c. This will be nonzero if, and only if, ring i is threaded by that strand of ring j. For instance, the two strands of the green ring in Figure 1b are threading the yellow ring, since the absolute value of the linking numbers of each of these (after closure) with the closed yellow loop are equal to one. We define the local threading of ring i by ring j in cell c at time t by $\mathrm{Th}_c(i, j; t) = 1/2 \sum_{j_c} |Lk(i_c, j_c; t)|$, equal to 1 for the example shown in Figure 1b, and the total threadings between these rings by summing this over all cells

$$\mathrm{Th}(i, j; t) = \sum_c \sum_{j_c} \frac{|Lk_c(i_c, j_c; t)|}{2} \tag{1}$$

This procedure is perfectly well-defined, even when rings enter and leave through the same faces of the cell (see also SI). We emphasize that this is taken to be a definition of threading. It is necessarily a strictly local measure, on the scale of the cell volume. If the cell volume is increased no threadings will eventually be recorded since rings in the melt are unlinked by construction.

We assign a passive threading of ring i by ring j when $\mathrm{Th}_c(i, j; t) = 1$ and $\mathrm{Th}_c(j, i; t) = 0$ and an active threading when $\mathrm{Th}_c(i, j; t) = 0$ and $\mathrm{Th}_c(j, i; t) = 1$. For example, in Figure 1b, the yellow ring is passively threaded by the green one, which is actively threading the yellow one.

The equilibrium average $\langle \mathrm{Th}_c(i, j; t) \rangle_{i,j,t}/N \equiv \langle \mathrm{Th} \rangle/N$ is the number of threadings per chain and is found to scale extensively with the ring length M. This may be related to the fact that the number of cells visited by each chain also grows linearly with M (see Figure 2).

We claim that the existence of these penetrations influences the dynamics of the rings by pinning chains' segments. A measure of this is given by their time-correlation function

$$P_p(t) = \left\langle \frac{\sum_j p(i, j; t_0) p(i, j; t_0 + t)}{\sum_j p(i, j; t_0)} \right\rangle_{i, t_0} \tag{2}$$

where $p(i, j; t) = 1$ if ring j is penetrating (threading) ring i at time t and 0 otherwise.

For large ring length M, $P_p(t)$ tends to flatten, resembling a plateau, before relaxing to a constant value $P_p(t \to \infty)$ $\langle p(i, j; t_0) \rangle_{i,j,t_0}$, this being the mean probability that two different, randomly chosen chains are penetrating. By using a mean-field argument, the probability of threading between two chains in any cell that they both occupy p_{th} can be approximated as the total probability that they thread divided by the number of shared cells that they both occupy N_{sc}
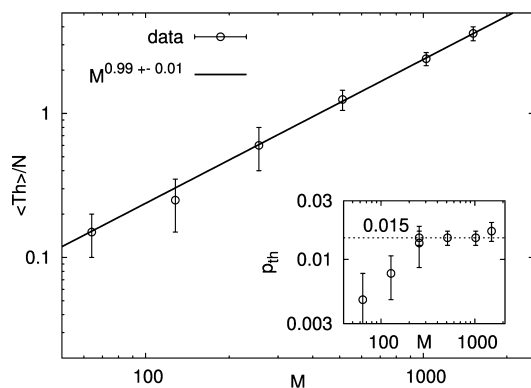
Figure 2. Number of threadings $\langle \text{Th} \rangle$ per chain as a function of the length of the chains M. In the inset we plot p_{th}, crudely the probability of threading in a cell containing two different chains, as computed in eq 3. See text for details.

$$p_{\text{th}} = P_{\text{p}}(t \to \infty)/N_{\text{sc}} \qquad (3)$$

We combine our measurement of N_{sc} and $P_{\text{p}}(t \to \infty)$ in order to compute p_{th}, which is plotted in the inset of Figure 2.

We now compare the relaxation of threading with that of the modulus $G(t)$ for the stress carried by the rings, here computed as

$$G(t) = \left\langle \frac{\sum_c g(i, c; t_0)g(i, c; t_0 + t)}{\sum_c g(i, c; t_0)} \right\rangle_{i,t_0} \qquad (4)$$

where $g(i, c; t) = 1$ if ring i visits cell c at time t and 0 otherwise. While $G(t)$ is a standard quantity in polymer science the rheological response of the rings will be "mixed" with that of the gel. This could lead to possible complications in isolating the rheological response of the rings alone. We therefore propose that diffusion of labeled tracer rings may be the most effective experimental probe of their dynamics. From the inset of Figure 3a it is clear that the spatial stress relaxes more quickly than the threadings. This is consistent with the fact that one ring, penetrated by another in any particular cell, can independently relax the stress it carries in all other cells. As reported previously,[6,9,15,27] the stress is found to relax faster than for melts of linear polymers, lacking any glassy plateau. Long-lived penetrations may be responsible for the fact that the segmental mean square displacement of a ring only starts to freely diffuse ($\langle \delta r_s^2 \rangle \sim t$) after the ring itself has moved many times R_g, see Figure 1c. This is in contrast to linear polymers, where there are no penetrations and the same crossover is on the order of R_g.[15] We infer that free diffusion can only occur when the most persistent penetrations have relaxed, on the time-scales shown in Figure 3a.

Figure 3b shows that chain reorientation is fast. For $M = 256$ it is comparable to the unthreading and diffusive relaxation times but it is much faster for $M \geq 512$. It may be significant that this is at the same point that significant clusters of interpenetrated rings start to appear, see Figure 4. These clusters do little to inhibit intrachain reorganization but the network of mutual pinning seems to be associated with the slowing of unthreading and diffusive relaxation. Figure 3b also shows that the diffusive relaxation time closely follows the unthreading time, supporting the hypothesis that free diffusion is possible only once the most persistent threadings are lost. In addition, we show that for the longest rings the penetrations relax much more slowly. We associate this with the emergence
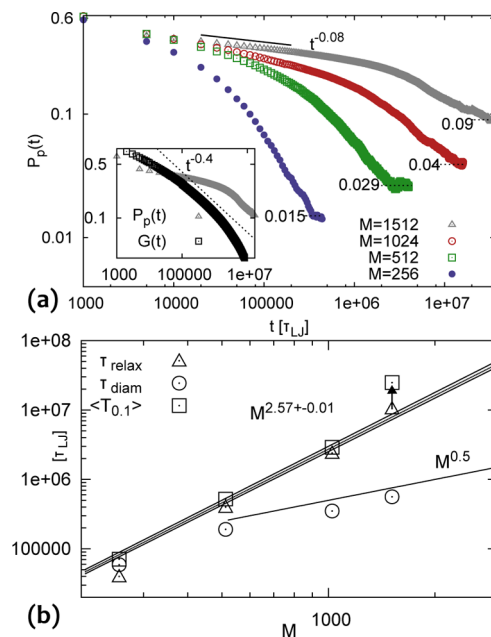

Figure 3. (a) Time-correlation function $P_{\text{p}}(t)$ of the penetrations as in eq 2. The inset compares the relaxation of the stress carried by the rings, through the modulus $G(t)$, with $P_{\text{p}}(t)$ for the system with longest rings showing that the spatial stress relaxes more quickly than the threadings. (b) Compares three dynamic relaxation times, defined as $\tau_{\text{relax}} \equiv \langle R_g^2 \rangle/6D_{\text{CM}}$, $\tau_{\text{diam}} \equiv \int_0^\infty C_{\text{diam}}(t)dt$ ($C_{\text{diam}}(t)$ is the time autocorrelation function of the diameter vector $\vec{d}(t)$ that joins opposite beads along the rings' contour (see SI for details)) and $\langle T_{0.1} \rangle$, given by the solution of $P_{\text{p}}(T_{0.1}) \equiv 0.1$. The arrow on top of the data point showing τ_{relax} for the longest rings $M = 1512$ indicates that this represents a lower bound: the crossover to diffusive motion has not yet occurred at the longest computationally accessible times. The unthreading times $\langle T_{0.1} \rangle$ for $M = 256$, 512, and 1024 follow the power law shown and are close to the corresponding values of τ_{relax}. The shaded region delimits the confidence bounds expected for the final data point for the unthreading time $\langle T_{0.1} \rangle$ at $M = 1512$, were it to continue to follow this power law. This point is approximately 30 standard deviations outside the confidence interval, consistent with a dramatic slowing-down due to the development of a strongly connected network of inter-ring penetrations (threadings).

of strongly connected components in the network of inter-ring penetrations, see Figure 4. This is consistent with Figures 2 and 3a, showing that, as we increase the length of the rings at fixed density, there is a corresponding increase in the number of threadings which also become more long-lived. In the percolating, long-lived cluster of interthreading rings that emerges the motion of each ring is strongly constrained by its passive threadings.

In order to quantify the network of penetrations, we define a directed graph $G = G(\mathcal{E}, \mathcal{V})$ where $\mathcal{V}$ is the set of vertices, a subset of the set of N rings in the system, and $\mathcal{E}$ is the set of directed edges from ring j to ring i, which represent the threadings of ring j through ring i. We keep track of the time-evolution of the network via the matrix $\text{Th}(i, j; t)$ and quantify the emergence of extended structures of interthreading rings by using the size of the largest strongly connected component $|N_{\text{scc}}|$ and the first Betti number $b_1(G)$ (see SI). As one can notice from Figure 4, most connected structures for short rings are formed by only two mutually threading rings while, for longer rings, these eventually contain $O(N)$ vertices, signifying the emergence of a percolating cluster of interpenetrating rings
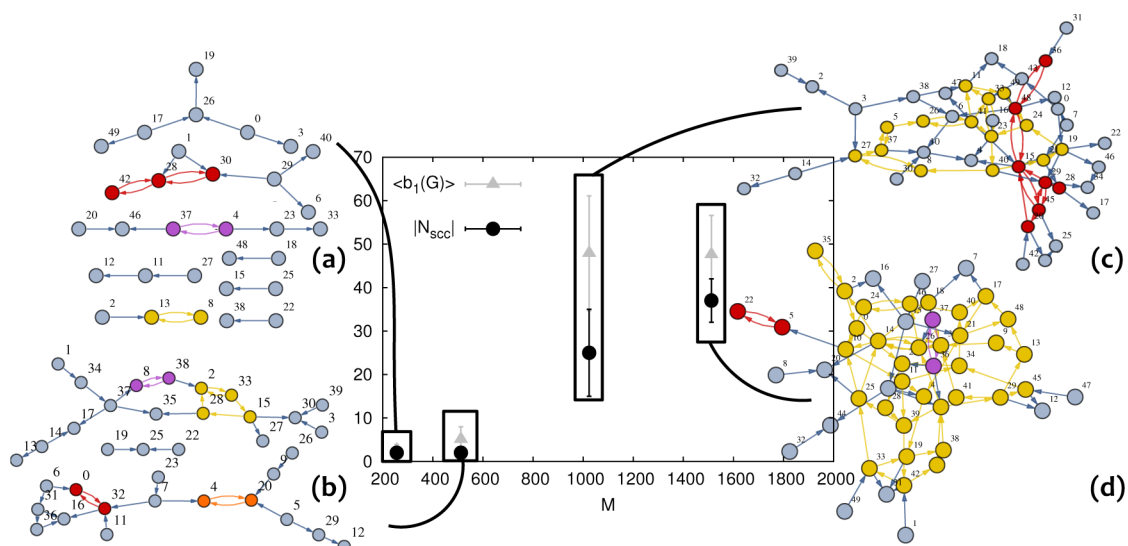
Figure 4. Betti number $b_1(G)$ (see SI) and size of the largest strong connected component $|N_{scc}(G)|$ computed taking the time average after equilibration. Snapshots of the graphs $G(\mathcal{E}, \mathcal{V})$ corresponding to $M = 256$ (a), 512 (b), 1024 (c), and 1512 (d) beads. The colors highlight the strongly connected components in the graphs (see text for details).

which scales with the size of the system. We claim that such static transition in the structure is related to a correspondent dynamic transition, whose effect can be observed in the significant deviation showed in Figure 3b.

In summary, we have employed a new method to quantify inter-ring threadings and to relate these to their dynamics in a background gel. Our findings suggest that inter-ring penetrations become more important as the length of the rings increases and that the dynamics of the polymers slows correspondingly. We highlight the existence of strongly connected components in the network of interpenetrating rings and show that such components grow as the length of the rings is increased with a cluster of size $O(N)$ interpenetrating rings emerging for the longest chains we study. Together with the result that $Th(M)/N \sim M$ we speculate that the dynamics is likely to be strongly suppressed for even longer rings. The term topologically jammed state might be used to describe this highly interpenetrated state of matter, which could have the unusual property that the dynamics could appear glassy, or at least slowed, well above the classical glass temperature T_g for the polymer itself and hence without appreciable loss of microscopic mobility. As the molecular weight of the ring polymers increases, the dynamics is expected to dramatically slow down due to the topology of the polymers, which must unthread one another in a particular order. This is rather different to the corresponding dynamics of linear polymers. This state would also inherit the well-known universality class of polymer physics and it would therefore seem to offer a novel framework in which to study a jamming transition from a topological perspective.

ASSOCIATED CONTENT

S Supporting Information

Additional computational and analytical details. This material is available free of charge via the Internet at http://pubs.acs.org.

AUTHOR INFORMATION

Corresponding Author

*E-mail: m.s.turner@warwick.ac.uk.

Notes

REFERENCES

(1) Everaers, R.; Sukumaran, S. K.; Grest, G. S.; Svaneborg, C.; Sivasubramanian, A.; Kremer, K. *Science* **2004**, *303*, 823–6.
(2) Doi, M.; Edwards, S. *The Theory of Polymer Dynamics*; Oxford University Press: Oxford, 1988.
(3) Gennes, P. D. *Scaling Concepts in Polymer Physics*; Cornell University Press: Ithaca, NY, 1979.
(4) Rubinstein, M. *Phys. Rev. Lett.* **1986**, *57*, 3023–3026.
(5) Grosberg, A. Y.; Rabin, Y. *Europhys. Lett.* **1993**, *23*, 373–378.
(6) Obukhov, S.; Rubinstein, M. *Phys. Rev. Lett.* **1994**, *73*, 1263–1266.
(7) Deutsch, J. *Phys. Rev. E* **1999**, *59*, 2539–2541.
(8) Muller, M.; Wittmer, J.; Cates, M. *Phys. Rev. E* **2000**, *61*, 4078–4089.
(9) Kapnistos, M.; Lang, M.; Vlassopoulos, D.; Pyckhout-Hintzen, W.; Richter, D.; Cho, D.; Chang, T.; Rubinstein, M. *Nat. Mater.* **2008**, *7*, 997–1002.
(10) Suzuki, J.; Takano, A.; Matsushita, Y. *J. Chem. Phys.* **2008**, *129*, 034903.
(11) Vettorel, T.; Grosberg, A. Y.; Kremer, K. *Phys. Biol.* **2009**, *6*, 025013.
(12) Sakaue, T. *Phys. Rev. Lett.* **2011**, *106*, 167802.
(13) Robertson, R. M.; Laib, S.; Smith, D. E. *Proc. Natl. Acad. Sci. U.S.A.* **2006**, *103*, 7310–7314.
(14) Robertson, R. M.; Smith, D. E. *Proc. Natl. Acad. Sci. U.S.A.* **2007**, *104*, 4824–4827.

(15) Halverson, J. D.; Lee, W. B.; Grest, G. S.; Grosberg, A. Y.; Kremer, K. *J. Chem. Phys.* **2011**, *134*, 204905.

(16) Klein, J. *Macromolecules* **1986**, *118*, 105−118.

(17) Halverson, J. D.; Lee, W. B.; Grest, G. S.; Grosberg, A. Y.; Kremer, K. *J. Chem. Phys.* **2011**, *134*, 204904.

(18) Lo, W.-C.; Turner, M. S. *Europhys. Lett.* **2013**, *102*, 58005.

(19) Bernabei, M.; Bacova, P.; Moreno, A. J.; Narros, A.; Likos, C. N. *Soft Matter* **2013**, *9*, 1287.

(20) Deutsch, J. *Science* **1988**, *456*, 16−18.

(21) Alon, U.; Mukamel, D. *Phys. Rev. E* **1997**, *55*, 1783−1793.

(22) Kremer, K.; Grest, G. S. *J. Chem. Phys.* **1990**, *92*, 5057.

(23) Fatin-Rouge, N.; Starchev, K.; Buffle, J. *Biophys. J.* **2004**, *86*, 2710−9.

(24) Um, S. H.; Lee, J. B.; Park, N.; Kwon, S. Y.; Umbach, C. C.; Luo, D. *Nat. Mater.* **2006**, *5*, 797−801.

(25) Park, N.; Um, S. H.; Funabashi, H.; Xu, J.; Luo, D. *Nat. Mater.* **2009**, *8*, 432−7.

(26) Lee, J.; Peng, S.; Yang, D.; Roh, Y. *Nat. Nanotechnol.* **2012**, *7*, 787−791.

(27) Pasquino, R.; et al. *ACS Macro Lett.* **2013**, *2*, 874−878.